

1. TITLE
2. INVESTIGATOR(S)
3. INTRODUCTION
4. THEORY OF ALGORITHM/MEASUREMENTS
5. EQUIPMENT
6. PROCEDURE
7. OBSERVATIONS
8. DATA DESCRIPTION
9. DATA MANIPULATIONS
10. ERRORS
11. NOTES
12. REFERENCES
13. DATA ACCESS
14. GLOSSARY OF ACRONYMS

1. TITLE

1.1 Data Set Identification

ISLSCP II Atmospheric Carbon Dioxide Consumption by Continental Erosion

1.2 Database Table Name(s)

Not applicable to this data set.

1.3 File Name(s)

Continental Flux: The continental flux data represent gridded estimates for the consumption of atmospheric CO₂ by continental erosion based on empirical models.

There are 2 data files *.zip, with this data set:

File Names:

continent_maps_1deg.zip: When extrapolated contains 5 *.asc files in standard ESRI ARCGIS GRIDASCII format, and are at 1.0 degree spatial resolution, containing 360 columns and 180 rows of data.

continent_maps_hdeg.zip: When extrapolated contains 6 *.asc and 6 *.dif files (total of 12 files). The *.asc files are in standard ESRI ARCGIS GRIDASCII format, and are at 0.5 degree spatial resolution, containing 720 columns and 360 rows. The *.dif files are differences files.

The .asc files, and file descriptions for both .zip files, are as follows, where XX is 1d or hd spatial resolution:

cont_flux_co2rw_XX_map.asc:	bicarbonate export (atmospheric origin), also called "atmospheric CO ₂ consumption by rock weathering"
cont_flux_doc_XX_map.asc:	dissolved organic carbon (DOC) export
cont_flux_hco3_XX_map.asc:	bicarbonate export
cont_flux_poc_XX_map.asc:	particulate organic carbon (POC) export

cont_flux_tss_XX_map.asc: sediment export

The .5 degree data **.dif** files have the same file names as above. These are ASCII table "difference" files (with an extension of "**.dif**") from each **xxxxx**-type map above.

There is also one changemap file included in the hdeg .zip file:

cont_flux_hd_changemap.asc shows the results of applying the land/water mask, as a viewable ASCII map: all points added (positive number, containing the "Interpolation_Level", see above), all points unchanged ("0"), and all points removed ("-1"). (see Sections 8.4 and 9.2.3 for more details).

In addition, the authors have provided graphical versions of their .5 degree resolution data for visualization purposes of oceanic flux, and this is also described in the documentation presented here. There are 11 GIF format files included as [companion files](#) and named with the same format as the continental and oceanic files with the exception that they end in the extension "**.gif**". An additional file showing the flow directions used in the river routing is also provided (**flow_dir.gif** file). All of these files can be viewed with most standard image display programs. The original oceanic flux data files (not provided with this data set) have a spatial resolution of 2.5 x 2.0 degrees lat/long.

1.4 Revision Date of this Document

June 27, 2011

2. INVESTIGATOR(S)

2.1 Investigator(s) Name and Title

Dr. Wolfgang Ludwig

Centre de Formation et de Recherche sur l'Environnement Marin (CEFREM)

Centre National de la Recherche Scientifique (CNRS)/ University of Perpignan, Perpignan, France

Dr. Philippe Amiotte-Suchet

Géochimie des Interfaces Sol-Eau / Centre des Sciences de La Terre

University of Bourgogne, Dijon, France

Dr. Jean-Luc Probst

Laboratoire des Mécanismes de Tranfert en Géologie

CNRS / University Paul Sabatier, Toulouse, France

2.2 Title of Investigation

A global evaluation of the atmospheric CO₂ consumption by continental erosion and the riverine fluxes of carbon and sediments to the oceans (carried out as a part of the EU research project ESCOBA (European Study of Carbon in the Ocean, Biosphere and Atmosphere), contract-no. ENV4-CT95-0111).

2.3 Contacts (For Data Production Information)

	Contact 1	Contact 2
2.3.1 Name	Dr. Wolfgang Ludwig	Dr. Philippe Amiotte-Suchet
2.3.2 Address	CEFREM / CNRS-Université de Perpignan 52, Av. de Villeneuve Perpignan 66860 Perpignan Cedex France	GéoSol / Université de Bourgogne 6, Bvd. Gabriel Dijon 21000 Dijon France
2.3.3 Tel. No.	+33 4 68 66 20 93	+33 3 80 39 39 71
Fax No.	+33 4 68 66 20 96	+33 3 80 39 63 87
2.3.4 E-mail	ludwig@univ-perp.fr	phamiots@u-bourgogne.fr

	Contact 3 (ISLSCP II)
2.3.1 Name	Mr. David Landis
2.3.2 Address	Code 614.4 NASA/GSFC Greenbelt, MD 20771 USA
2.3.3 Tel. No.	(301) 286-3349
Fax No.	(301) 286-0239
2.3.4 E-mail	david.r.landis@gsfc.nasa.gov

2.4 Data Set Citation

Ludwig, W., P. Amiotte-Suchet, J.L. Probst . 2011. ISLSCP II Atmospheric Carbon Dioxide Consumption by Continental Erosion. In Hall, Forrest G., G. Collatz, B. Meeson, S. Los, E. Brown de Colstoun, and D. Landis (eds.). ISLSCP Initiative II Collection. Data set. Available on-line [<http://daac.ornl.gov/>] from Oak Ridge National Laboratory Distributed Active Archive Center, Oak Ridge, Tennessee, U.S.A. [doi:10.3334/ORNLDAAC/1019](https://doi.org/10.3334/ORNLDAAC/1019)

2.5 Requested Form of Acknowledgment

Users of the International Satellite Land Surface Climatology (ISLSCP) Initiative II data collection are requested to cite the collection as a whole (Hall et al. 2006) as well as the individual data sets. Please cite the following publications when these data are used:

Hall, F.G., E. Brown de Colstoun, G. J. Collatz, D. Landis, P. Dirmeyer, A. Betts, G. Huffman, L. Bounoua, and B. Meeson, The ISLSCP Initiative II Global Data sets: Surface Boundary Conditions and Atmospheric Forcings for Land-Atmosphere Studies, *J. Geophys. Res.*, 111, doi:10.1029/2006JD007366, 2006.

Amiotte-Suchet, P. and Probst, J.L., 1995a. A global model for present day atmospheric/ soil CO₂ consumption by chemical erosion of continental rocks (GEM-CO₂). *Tellus*, 47B, 273-280.

Ludwig, W., Probst, J.-L., and Kempe, S. (1996a). Predicting the oceanic input of organic carbon by continental erosion. *Global Biogeochemical Cycles*, 10, p. 23-41.

3. INTRODUCTION

3.1 Objective/Purpose

The erosion of the continents represents a permanent transfer of carbon from the atmosphere to the oceans by rivers. This process is also called the atmospheric CO₂ consumption by continental erosion. The purpose of this study is to understand the controls for this carbon transfer and to develop global and regional budgets in order to evaluate the importance of this transport pathway within the global carbon cycle. Previous modeling studies on the fate of the anthropogenic released CO₂ often revealed an inconsistency of the observed latitudinal CO₂ gradient in the atmosphere with the predicted transport fields. Up to now, however, it was difficult to include the fluvial carbon transport in models on the global carbon cycle because of the lack of sufficient river data worldwide. Our data may help to close this data gap. Moreover, a better knowledge of the present-day controls of the carbon fluxes related to continental erosion may also help to understand the behavior of the carbon cycle under different scenarios of global change, either for future scenarios or for the reconstruction of the geochemical and paleoclimatic history of the Earth during geological times.

3.2 Summary of Parameters

Continental erosion consumes atmospheric CO₂ via two major processes: the organic matter fixation in the biosphere and the subsequent erosion of this carbon, and by the chemical weathering of rocks, releasing bicarbonate ions (HCO₃⁻) into the soil solutions. The carbon is then transferred as dissolved organic carbon (DOC), particulate organic carbon (POC), and dissolved inorganic carbon (DIC) to the oceans by rivers. For all of these carbon fluxes, we determined the major controlling factors at the global scale, and established empirical regression models, which allowed an extrapolation of the fluxes to the overall continental area on the basis of global data sets for the controlling factors. Because the particulate organic carbon fluxes are strongly coupled to the fluxes of total suspended sediments (TSS), we also applied our approach to the fluxes of this key parameter at the global scale. Within the DIC fluxes, the carbon being of atmospheric origin was distinguished from the carbon being of lithological origin. Consequently,

five global data sets representing gridded estimates for the riverine export of carbon and of sediments on the continents have been created in a 0.5 degree by 0.5 degree longitude/ latitude grid point resolution (DOC, POC, TSS, DIC-atmosphere, DIC-total). This data has also been averaged into a set of 1.0 by 1.0 degree maps based on the 0.5 by 0.5 degree maps files.

3.3 Discussion

To provide consistency across the many data sets of the ISLSCP II data collection, the data sets provided here have been made consistent, when appropriate, with the land/water boundaries of the ISLSCP II data collection. Some points have been removed or added through interpolation but are provided in separate files for the user to reconstruct the original data. The description that follows provides information on the development of the original data sets by the authors.

History of the Data Set Development and Publications

The data sets we created are the result of previous studies on the river fluxes of inorganic carbon (Amiotte-Suchet and Probst, 1993a, b, 1995; Amiotte-Suchet, 1995a, b; Amiotte-Suchet et al., submitted), on the river fluxes of organic carbon (Ludwig et al., 1996a; Ludwig, 1997), and on the river fluxes of total suspended solids (Ludwig and Probst, 1996, 1998). These studies allowed establishing a series of empirical relationships that form together our Global Erosion Model for the atmospheric CO₂ consumption by continental erosion, GEM-CO₂ (Amiotte-Suchet, 1995, Ludwig et al., 1998). The coupling of GEM-CO₂ with a river routing file to determine the carbon penetration in the oceans has been published by Ludwig et al. (1996b), and two applications of GEM-CO₂ were done to simulate the atmospheric CO₂ consumption during the last glacial maximum by Ludwig et al. (1999), and by Ludwig and Probst (1999). Moreover, a coupling of our data sets with global atmospheric and oceanic transport models in order to evaluate the role of the river carbon for the interhemispheric transport of carbon can be found in Aumont et al. (2001).

Scientific Approach and Model Development

Concerning inorganic carbon, GEM-CO₂ is based on a data set of runoff and bicarbonate concentrations in 232 monolithologic watersheds in France that have been analyzed and published by Meybeck (1986). Empirical relationships between specific bicarbonate fluxes and runoff intensity were determined for the major rock types on Earth. The applicability of these relationships at the global scale was then validated on the level of large river basins, by comparing the modeled values to the observed fluxes. Concerning the fluxes of organic carbon and of sediments, the empirical relationships are based on a set of major world rivers. The hydroclimatic, biological, geomorphological, and lithological characteristics of the drainage basins are extracted from a large number of environmental data sets using the digitized basin contours. These characteristics are then used for statistical analyses together with literature data for these rivers on the observed fluxes of organic carbon and sediments. Most of the field data we used to establish the empirical relationships for the fluxes of organic carbon have been collected within the SCOPE/UNEP program Transport of Carbon and Minerals in Major World Rivers (for a summary, see Degens et al., 1991). All data sets we present were created by applying GEM-CO₂ to the total continental area on the basis of global data sets for the controlling factors. The empirical relationships and the data sets we used for the controlling factors are described in Sections 4, 6 and 9.

Global and Regional Budgets for the Continental Data Sets

According to our data, continental erosion represents a total sink for atmospheric CO₂ of about 0.60 GtC yr⁻¹. In this value, 0.21 GtC yr⁻¹ can be attributed to DOC fluxes (F_{DOC}), 0.16 GtC yr⁻¹ to POC fluxes (F_{POC}), and 0.23 GtC yr⁻¹ to bicarbonate fluxes released by rock weathering (F_{CO₂-RW}). Bicarbonate that originates from carbonate dissolution (F_{CARB}) makes an additional flux of 0.09 GtC yr⁻¹. The corresponding fluxes of water and of sediments are 41750 km³ yr⁻¹ and 16 Gt yr⁻¹, respectively. These values agree well with other literature estimates, confirming the applicability of GEM-CO₂ to the global scale (see Amiotte-Suchet and Probst (1995), Ludwig et al. (1996a), and Ludwig and Probst (1998) for a literature review of global inorganic carbon, organic carbon and sediment fluxes, respectively). In Table 1, regional budgets are given for all of these fluxes with respect to the major climates, different continents, and different ocean basins.

For all carbon forms, the tropical wet climate is the most important climate type with respect to the global fluxes. This points out the important role of drainage intensity for the consumption of atmospheric CO₂ by continental erosion. From the wet tropics originate 54.9 % of total F_{CO₂-RW}, 43.4 % of total F_{POC}, and 49.6% of total F_{DOC}. Runoff from the tropics accounts for 54 % of global runoff. The relative importance of F_{CO₂-RW} with respect to the total CO₂ consumption (F_{CO₂}; F_{CO₂}= F_{CO₂-RW} + F_{DOC} + F_{POC}) increases in regions where carbonate and shale outcrops are abundant. These rock types have high specific consumption rates (see below). The fact that the tropical wet climate is more important for F_{CO₂-RW} than for F_{DOC} and F_{POC} is related to the great abundance of shales in the Amazon basin and in Oceania. Carbonate outcrops are especially important between the latitudes 20 degrees and 40 degrees N. This is reflected in the values for the temperate wet climate type in Table 1, where the inorganic carbon fluxes are enhanced compared to the organic carbon fluxes. Nevertheless, the influence of lithology on F_{CO₂-RW} is naturally more evident at continental and regional scales. Note, for example, that for Africa the specific F_{CO₂-RW} value is about five times smaller than for South America (but the specific drainage intensity is only three times smaller). In Africa, plutonic and metamorphic rocks as well as sandstones are abundant over large areas. Because these rock types consume small amounts of atmospheric CO₂ (see below), this continent has low specific F_{CO₂-RW} values.

By far the greatest specific F_{CO₂-RW} values are observed in the south and southeast of Asia, where large carbonate outcrops coincide with great drainage intensities. This makes Asia to the continent with the highest specific F_{CO₂-RW} value. We calculated that about 23 % of global F_{CO₂-RW} takes place in the region of Asia between 75 degree to 135 degree E and 10 degree to 40 degree N, although this region covers only about 9 % of the total exoreic continental area. At the same time, the south and southeast of Asia is of similar importance for the fluxes of particulate organic carbon because of the great sediment delivery from this part of the world. About 25 % of global F_{POC} is discharged to the oceans from the above-specified region. This underlines the important role of this region with respect to the CO₂ consumption by continental erosion as far as the fluxes of bicarbonate and of POC are concerned. For F_{DOC}, only about 13 % of the global flux comes from the same region. Finally, one has also to notice that by far the major part of the atmospheric CO₂ consumption by continental erosion takes place in the Northern Hemisphere. According to our values, this is about 0.42 GtC yr⁻¹, or 70% of the global F_{CO₂} value.

Table 1-Regional budgets for the atmospheric CO₂ consumption by continental erosion and for river carbon fluxes to the oceans.

	Area * (10 ³ km ²)	FDOC (TgC/yr)	FPOC (TgC/yr)	FCO ₂ -RW (TgC/yr)	FCARB (TgC/yr)	Runoff (km ³ /yr)	Sediments (Tg/yr)
Polar (no ice)	3892	3.1	1.0	3.4	1.4	762	0.032
Tundra and Taiga	23232	45.9	15.0	33.0	8.6	6930	0.646
Temperate Dry	9635	2.9	12.5	4.3	2.0	729	2.403
Temperate Wet	16918	35.4	32.7	47.7	24.6	7753	3.300
Tropical Dry	21790	16.0	27.8	14.9	5.4	3101	4.520
Tropical Wet	24919	101.7	68.5	126.3	47.7	22403	5.090
Desert	5940	0.3	0.3	0.4	0.2	66	0.044
Total	106326	205.2	157.9	230.0	90.1	41744	16.035
Africa	18288	20.0	10.7	11.5	4.9	4120	0.973
Europe	9564	16.6	10.5	18.5	7.3	3079	0.841
North America	23020	39.4	27.6	40.5	17.2	7142	3.138
South America	17732	51.8	34.3	52.8	8.0	11150	2.940
Asia	32518	73.0	71.6	104.3	52.7	15318	7.930
Australia	4476	3.9	3.0	2.2	0.1	773	0.205
Antarctic Continent	728	0.6	0.2	0.1	0.1	162	0.007
Total	106326	205.2	157.9	230.0	90.1	41744	16.035
Arctic Ocean	16982	24.9	6.2	20.6	6.3	3239	0.235
North Atlantic	27300	71.0	39.3	71.9	22.6	13484	3.600
South Atlantic	16959	25.7	9.4	15.6	4.9	5074	0.523
Pacific	21025	57.0	68.6	79.6	31.9	13532	7.407
Indian Ocean	16594	21.4	28.1	32.9	19.6	5166	3.556
Mediterranean	6739	4.6	6.1	9.4	4.6	1087	0.708
below 60° South	728	0.6	0.2	0.1	0.1	162	0.007
Total	106326	205.2	157.9	230.0	90.1	41744	16.035

* Calculated without endoreic regions and regions that are under permanent ice cover

Global and Regional Budgets for the Oceanic Data Sets

When looking at the spatial distribution of the river carbon into the world's oceans (Table 2), the difference between the two hemispheres is even more important: more than 83 % of the overall river carbon ($F_{\text{DOC}} + F_{\text{POC}} + F_{\text{HCO}_3}$, with $F_{\text{HCO}_3} = F_{\text{CO}_2\text{-RW}} + F_{\text{CARB}}$) enters the sea in the Northern Hemisphere. Globally, 43% of the river carbon is injected in the Atlantic Ocean, 34% in the Pacific Ocean, 15% in the Indian Ocean, and 8% in the Arctic Ocean. Note that about 28% is discharged from the 10 greatest world river basins only, and more than one third (37%) of the carbon input into the Atlantic Ocean occurs in the 0-4 degrees N latitude band, where the mouth of the Amazon River is situated.

The general pattern is similar for the three carbon species because for all of them, the fluxes are strongly coupled to the spatial distribution of the freshwater inputs into the oceans. Differences are found, however, at local scales. Mainly the ratio ($R_{\text{DIC/TOC}}$) of inorganic (F_{HCO_3}) to organic ($F_{\text{DOC}} + F_{\text{POC}}$) carbon can vary considerably. The variability of the fluxes of organic carbon is more closely coupled to the variability of drainage intensity compared to the variability of the alkalinity fluxes. The latter are also strongly dependent on the outcropping rock types on the continents. Consequently, $R_{\text{DIC/TOC}}$ follows more or less the distribution of lithology. Especially large carbonate outcrops in river basins lead to great $R_{\text{DIC/TOC}}$ values in the ocean grid

Table 2 - River fluxes of carbon to the world's oceans. All values are in $TgC yr^{-1}$.

	Arctic Ocean			Atlantic Ocean (1)			Indian Ocean			Pacific Ocean		
Latitude	HCO ₃ ⁻	DOC	POC	HCO ₃ ⁻	DOC	POC	HCO ₃ ⁻	DOC	POC	HCO ₃ ⁻	DOC	POC
84-88 N	0.10	0.01	0.01	--	--	--	--	--	--	--	--	--
80-84 N	0.12	0.05	0.03	0.07	0.01	0.01	--	--	--	--	--	--
76-80 N	5.34	1.45	0.48	0.06	0.01	0.02	--	--	--	--	--	--
72-76 N	12.72	14.25	2.72	0.63	0.10	0.05	--	--	--	--	--	--
68-72 N	8.05	7.77	3.06	0.04	0.10	0.02	--	--	--	--	--	--
64-68 N	1.31	1.53	0.28	1.08	1.37	0.63	--	--	--	--	--	--
60-64 N	--	--	--	0.84	3.64	0.59	--	--	--	2.81	1.96	1.45
56-60 N	--	--	--	5.02	8.98	1.78	--	--	--	4.20	3.69	3.83
52-56 N	--	--	--	4.27	5.07	0.60	--	--	--	2.75	5.05	3.08
48-52 N	--	--	--	9.99	4.38	1.15	--	--	--	1.98	1.46	1.26
44-48 N	--	--	--	5.36	2.56	1.48	--	--	--	1.56	0.92	0.76
40-44 N	--	--	--	10.30	2.34	3.07	--	--	--	2.00	0.96	1.16
36-40 N	--	--	--	3.63	1.09	1.50	--	--	--	1.09	1.27	6.46
32-36 N	--	--	--	1.49	1.40	1.11	--	--	--	1.29	1.51	2.08
28-32 N	--	--	--	8.67	5.46	4.07	--	--	--	27.94	4.12	7.76
24-28 N	--	--	--	0.66	0.52	0.35	2.25	0.13	1.83	3.52	0.92	0.98
20-24 N	--	--	--	4.57	0.78	2.21	1.56	0.31	1.07	11.35	2.17	2.92
16-20 N	--	--	--	1.32	0.44	0.42	11.01	7.72	10.22	2.77	1.62	1.81
12-16 N	--	--	--	2.72	2.75	4.18	16.38	4.87	7.92	2.42	0.68	4.44
08-12 N	--	--	--	4.95	6.85	6.36	4.13	1.30	1.35	7.58	3.76	3.97
04-08 N	--	--	--	1.00	2.48	1.16	2.57	0.61	0.47	3.96	2.60	2.68
00-04 N	--	--	--	48.36	36.20	20.22	0.43	0.82	0.76	11.35	6.10	5.78
00-04 S	--	--	--	2.92	1.47	0.84	0.41	0.20	0.78	7.19	5.43	3.61
04-08 S	--	--	--	7.09	6.81	1.53	4.93	1.83	1.29	2.64	1.14	1.52
08-12 S	--	--	--	0.75	0.52	0.18	0.53	0.32	0.41	10.77	2.84	3.69
12-16 S	--	--	--	0.05	0.13	0.02	1.43	1.96	1.38	0.20	0.08	0.19
16-20 S	--	--	--	0.76	0.42	0.17	1.14	0.65	0.44	0.04	0.20	0.21
20-24 S	--	--	--	0.08	0.27	0.14	0.60	0.76	0.74	0.07	0.22	0.23
24-28 S	--	--	--	0.05	0.17	0.08	0.22	0.20	0.35	0.09	0.13	0.10
28-32 S	--	--	--	0.50	0.71	0.83	0.02	0.04	0.07	0.01	0.01	0.02
32-36 S	--	--	--	3.76	4.60	1.44	0.01	0.02	0.09	0.16	0.19	0.32
36-40 S	--	--	--	0.04	0.09	0.02	0.20	0.47	0.44	0.79	1.09	0.99
40-44 S	--	--	--	0.12	0.16	0.06	0.03	0.07	0.03	0.87	1.52	1.18
44-48 S	--	--	--	0.01	0.01	0.01	--	--	--	0.68	2.12	1.72
48-52 S	--	--	--	0.32	0.97	0.72	--	--	--	0.07	0.35	0.07
52-56 S	--	--	--	0.13	0.19	0.14	--	--	--	0.16	0.42	0.26
Total	27.64	25.06	6.58	131.61	103.05	57.16	47.85	22.28	29.64	112.31	54.53	64.53

(1) Including the Mediterranean Sea and the Black Sea

elements to which the rivers discharge. Because of carbonate rich watersheds of certain rivers discharging to these zones, $R_{DIC/TOC}$ values of 1.5 to more than 2 can be found, for example, in the Atlantic Ocean in the latitude bands of 48-52 degrees N (e.g., the St. Lawrence River) and of 40-44° N (some European rivers such as the Rhône River), or in the Pacific Ocean in the 28-32 degrees N (e.g., the Changjiang River) and in the 20-24 degrees N (e.g., the Hungho River) latitude bands. On the continents, carbonate outcrops are mainly abundant in the Northern Hemisphere, such as in Southeast Asia, in Western Europe, or in the eastern United States. For this reason, $R_{DIC/TOC}$ is greater in the parts of the oceans north of the equator than south of it. Greatest average values are found in the North Pacific ($R_{DIC/TOC} = 0.99$) and in the northern

Indian Ocean ($R_{\text{DIC}/\text{TOC}} = 0.97$). In the South Atlantic and in the southern Indian Ocean, the ratios of inorganic to organic river carbon inputs are low ($R_{\text{DIC}/\text{TOC}} = 0.73$ and 0.76 , respectively).

With respect to the two organic carbon forms, DOC and POC, the inputs of DOC are dominant in the Atlantic Ocean. The DOC to POC ratio, $R_{\text{DOC}/\text{POC}}$, is on average 1.7 in the North Atlantic, and 2.7 in the South Atlantic. Particulate organic carbon inputs are more abundant in the Pacific and in the Indian Ocean. In the northern Indian Ocean, the share of POC in the organic matter fluxes is greatest ($R_{\text{DOC}/\text{POC}} = 0.7$ on average) because of the great sediment fluxes that are characteristic for the rivers draining the South and Southeast of the Himalayan region (e.g., the Ganges/ Brahmaputra, Indus, and Irrawaddy rivers). By far the greatest average $R_{\text{DOC}/\text{POC}}$ value is found for the Arctic Ocean. Mechanical erosion rates are very small in the boreal climate zones (Table 1) and the soils are generally rich in organic carbon. This is leading to elevated DOC fluxes (see below). Nearly 80% of the total organic carbon input occurs here in the dissolved form ($R_{\text{DOC}/\text{POC}} = 3.8$).

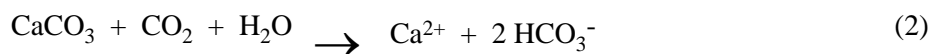
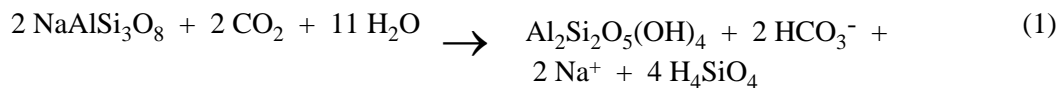
4. THEORY OF ALGORITHM/MEASUREMENTS

In this part, we outline the empirical relationships between the different environmental parameters defining our model GEM-CO₂. The corresponding equations and the description of the data sources are given in Sections 9 and 6, respectively.

4.1 Inorganic Carbon

Concerning inorganic carbon, it could be shown that the riverine fluxes are mainly a function of drainage intensity and of the rock type that is drained by the surface waters (Amiotte-Suchet, 1993a, b; 1995a, b; Amiotte-Suchet, 1995). In our model, the watersheds were grouped into six lithological classes representative for the major rock types outcropping on the continents, and the empirical relationships between specific bicarbonate fluxes (F_{HCO_3}) and drainage intensity (Q) were determined for each of the six classes. A linear relationship was found for each rock type. For a given runoff intensity, F_{HCO_3} varies considerably for different rock types. F_{HCO_3} are more than 30 times greater for carbonate rocks, the rock type with the greatest weathering rate, than for plutonic and metamorphic rocks, the rock type with the lowest weathering rate. In the order of decreasing weathering rates, the six rock types can be classified as follows: carbonate rocks, shales, basalts and gabbros, acid volcanic rocks, sands and sandstones, and plutonic and metamorphic rocks.

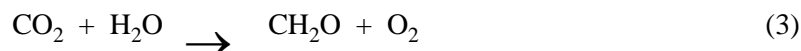
According to the stoichiometry of the weathering reactions, the atmospheric CO₂ consumption by rock weathering ($F_{\text{CO}_2\text{-RW}}$) was considered to be equal to the bicarbonate fluxes in waters draining silicate rocks, and to be equal to half of the bicarbonate fluxes in waters draining carbonate rocks. This can be seen, for example, by comparing the equations for the albite hydrolysis (eq. 1) and the calcite dissolution (eq. 2):



4.2 Organic Carbon

Concerning the fluxes of organic carbon, empirical relationships have been established on a set of major world rivers. It was found that a multiple regression model including drainage intensity, basin slope, and the amount of carbon stored in the soils is the best model to predict the specific DOC fluxes (F_{DOC}) on a global scale (Ludwig et al., 1996a; Ludwig, 1997). They become greater with increasing drainage intensities, flatter morphologies, and larger carbon reservoirs in the soils. For POC, sediment fluxes are the dominant controlling parameter. It could be shown that the specific POC fluxes (F_{POC}) generally increase with increasing sediment fluxes, but the percentage of organic carbon in the total suspended solids clearly decreases with increasing sediment concentrations. This relationship was mathematically fitted, allowing calculating the POC fluxes to the oceans as a function of sediment yields (specific sediment fluxes) and of drainage intensity.

For the atmospheric CO_2 consumption associated with the erosion of organic carbon, we assumed that all of the organic carbon in rivers is of atmospheric origin. This can be seen when looking at the photosynthesis reaction, which can be written in a simplified form as following:



Only the part of fossil DOC and POC that is mobilized with the erosion of organic rich sedimentary rocks may be distinguished here from the bulk POC because of its much older age. In our approach we considered that this carbon is only of minor importance and no distinction between recent and fossil organic matter was done (Ludwig et al, 1996).

4.3 Sediment Fluxes

For the modeling of sediment yields, we found that the fluxes (F_{TSS}) could be best correlated by forming the products of hydroclimatic and geomorphological factors, that is runoff intensity, basin slope, an index characterizing rock hardness, and an index characterizing rainfall variability over the year (Ludwig and Probst, 1996 1998). The best parameter combination varies to some extent when the rivers are grouped according to their average climatic situation, but it is always a combination of the above-mentioned parameters that yields the most significant models. In arid climates, however, regression coefficients are greater than in humid climates, indicating that erodibility is much greater in arid climates.

5. EQUIPMENT

This section is not applicable to our data sets. All data we produced are model outputs.

5.1 Instrument Description

5.1.1 Platform (Satellite, Aircraft, Ground, Person)

Not applicable to this data set.

5.1.2 Mission Objectives

Not applicable to this data set.

5.1.3 Key Variables

Not applicable to this data set.

5.1.4 Principles of Operation

Not applicable to this data set.

5.1.5 Instrument Measurement Geometry

Not applicable to this data set.

5.1.6 Manufacturer of Instrument

Not applicable to this data set.

5.2 Calibration

5.2.1 Specifications

5.2.1.1 Tolerance

Not applicable to this data set.

5.2.2 Frequency of Calibration

Not applicable to this data set.

5.2.3 Other Calibration Information

Not applicable to this data set.

6. PROCEDURE

6.1 Data Acquisition Methods

The scientific approach leading to the creation of our data requires using other global data sets for different climatic, biological, morphological and lithological parameters (lower level data sets). On the one hand, these data sets were needed for a detailed characterization of the mean environmental patterns of the river basins, which were then used to perform the regression statistics together with independent literature estimates for the investigated river fluxes (except for the fluxes of dissolved inorganic carbon). On the other hand, the data sets for the corresponding controlling factors were needed to apply GEM-CO₂ to the overall continental area. Table 3 lists the global environmental data sets we considered in our studies. Bold parameters are those that are necessary to run GEM-CO₂ (see Section 9). These data sets are described below:

Annual Drainage Intensity and Precipitation

Both the global distributions of mean annual drainage intensity and mean annual precipitation were digitized following the contour lines on the original maps created by Korzoun et al. (1977) for each of the Earth's continents. The inversion of these maps, i.e. the conversion of

Table 3 – Environmental data sets considered in this study (bold parameters are needed to run GEM-CO₂).

Parameter Group	Environmental Parameter	Abbreviation	Resolution	Source
hydroclimatic parameters	monthly and annual temperature mean (°C)	MT, AT	0.5 degree x 0.5 degree	Legates & Willmott, 1992
	monthly and annual precipitation total (mm)	MPPT, APPT	0.5 degree x 0.5 degree	Korzoun and others, 1977; Legates and Willmott, 1992; Ludwig et al., 1998
	mean annual runoff intensity (mm)	Q	0.5 degree x 0.5 degree	Korzoun and others, 1977; Ludwig et al., 1998
	seasonal precipitation variability (mm)	Four	0.5 degree x 0.5 degree	CORINE, 1992; Fournier, 1960
	aridity Index	ArIn	0.5 degree x 0.5 degree	CORINE, 1992
	major climate type	Clim	0.5 degree x 0.5 degree	Holdridge, 1947, 1964, Ludwig et al., 1996a
biological parameters	biomass density (kg/m ²)	VegC	0.5 degree x 0.5 degree	Olson et al., 1983; 1985
	net primary production (kg/m ²)	NPP	0.5 degree x 0.5 degree	Olson et al., 1983; 1985
	forest ratio (% of all vegetation types / 100)	ForR	0.5 degree x 0.5 degree	Olson et al., 1983; 1985; Claussen and others, 1994
	organic carbon content in the soils (kg/m ³)	SoilC	10' x 10'	USDA Soil Conservation Service, pers. com.
pedological parameters	average soil depth (cm)	SoilH	1.0 degree x 1.0 degree	Webb et al., 1991
	average soil texture	SoilTI	1.0 degree x 1.0 degree	Webb et al., 1991; CORINE, 1992
morphological parameters	modal basin elevation (m), maximum basin elevation (m)	Elev, ElevM	10' x 10'	FNOC, 1992
	local relief (m)	LR	10' x 10'	FNOC, 1992; Ahnert, 1970
	surface slope (radian)	Slope	5' x 5'	Moore and Mark, 1986
lithological parameters	spatial distribution of major rock types	Lith	1.0 degree x 1.0 degree	Amiotte Suchet, 1995 ; Amiotte-Suchet et al., submitted
	chemical erodibility index	LithCI	1.0 degree x 1.0 degree	Amiotte Suchet, 1995
	mechanical erodibility index	LithMI	1.0 degree x 1.0 degree	Probst, 1992
anthropogenic parameters	mean population density (h/km ²)	PopD	2.5 degrees x 2.5 degrees	Ahamer and others, 1992

	percent of cultivated area (%)	CultA	0.5 degree x 0.5 degree	Olson et al., 1983; 1985
--	--------------------------------	-------	-------------------------	--------------------------

the rectangular Cartesian coordinates of the contour lines into a longitude-latitude coordinate system, is a non-linear problem. It has been solved iteratively with a Nelder-Mead downhill simplex method applied to the nodes of the grid, combined with a least squares procedure. To minimize errors, each map grid was read in at least twice, but generally four times. The contour lines were then interpolated on a regular longitude-latitude 0.25 degrees x 0.25 degrees grid using a Delaunay triangulation method, and reduced to a final version in a 0.5 degrees x 0.5 degrees resolution. This method yields a specific annual runoff value of 332 mm for the total continental area, and a specific annual precipitation value of 817 mm. This is 3% and 2% greater than the estimates given by Korzoun et al. (1977), respectively. For precipitation, there is a similar agreement when looking at the mean values for 10 degree latitudinal bands (for runoff, the authors do not give the latitudinal distribution). Deviation is also in the range of a few percent only, except for the band stretching over the southern tip of South America, which may be due to differences in the area estimates.

Monthly Precipitation and Fournier Index

Mean monthly precipitation has been derived from the data set of Legates and Willmott (1992) by transforming their values to the percentages of the annual totals, and by applying these values to the annual precipitation data set we created from the maps of Korzoun et al., 1977 (see above). This was done because the precipitation data of Korzoun et al. (1977) are in better agreement with the data for drainage intensity. Seasonal variability of precipitation was characterized by calculating the sum of the square of mean monthly precipitation over mean annual precipitation for all 12 months of the year (according to CORINE, 1992). This parameter was named “Four”. Fournier (1960) proposed a very similar index, although he only selected the ratio of the square of precipitation of the month with the greatest value over the annual precipitation total.

Major Climate Types

All climatic distinctions in GEM-CO₂ are bases on the Holdridge Life Zone diagram. This diagram was originally proposed to relate the character of natural vegetation associations to climatic indices (Holdridge, 1947; 1964). Life zones are depicted by a series of hexagons formed by intersecting intervals of climate variables on logarithmic axes in a triangular coordinate system. Two variables, the average biotemperature (ABT) and the mean annual precipitation total (APPT), uniquely determine the classification. ABT is the average annual temperature with negative temperatures set to zero. The third variable in the diagram, the annual potential evapotranspiration ratio (APETR), is the ratio of mean annual potential evapotranspiration (APE) over mean annual precipitation. Since APE is calculated as a linear function of ABT (the constant of proportionality is 58.93), APETR directly depends on the two primary variables ABT and APPT.

The following climate types were created, using the hexagon lines and not the straight intersect lines as boundary lines: (1) polar, with ice = ABT < 1.5 °C and under permanent ice cover; (2) polar, without ice = ABT < 1.5 degrees C and without permanent ice cover; (3) deserts = bioclimates with APETR > 4.0; (4) temperate dry = bioclimates with 6.0 °C < ABT < 17.0 degrees C and 4.0 > APETR > 1.0; (5) tundra and taiga = bioclimates with 1.5°C < ABT < 6.0

degrees C; (6) tropical dry = bioclimates with $ABT > 17$ degrees C and $4.0 > APETR > 1.0$; (7) temperate wet = bioclimates with 6.0 degrees C $< ABT < 17.0$ degrees C and $APETR < 1.0$; (8) tropical wet = bioclimates with $ABT > 17$ degrees C and $APETR < 1.0$. This classification forms the basis of all climatic considerations that were made in the model. Note that the intersect $APETR = 1$ divides dry and wet climate types. Dry climate types are hence water limited with respect to their annual means, while there is an excess of water in the wet climate types. Only for the tundra and taiga climate type we did not apply such a distinction. This is because dry regions in this climate type are very rare in nature (only about 0.5% of the total exoreic tundra and taiga area would fall in dry bioclimates).

Soil Organic Carbon Storage

The mean organic carbon content in the soils (SoilC) was extracted from a global data set developed in a 10' by 10' longitude/ latitude resolution at the Soil Conservation Service of the United States Department of Agriculture (USDA-SCS). They kindly made it available for us. We averaged it to a resolution of 0.5 degree by 0.5 degree longitude/ latitude. In this data set, the average amount of soil carbon was empirically determined for each soil type to the suborder level in soil taxonomy on the basis of a database maintained at the USDA-SCS, and then extrapolated to the global scale using the FAO soil maps of the world (FAO, 1971-81). It is assumed that all organic carbon in soils is concentrated in the first meter of the soil profile. The USDA-SCS database is described in Eswaran et al. (1993) and in Kern (1994). From this newly created data set, we calculated the global amount of carbon stored in the soils to be 1470 GtC, which is in good agreement with other estimates (e.g. Post, 1993).

Steepness of Morphology

For the characterization of the steepness of morphology (slope), we used the mean grid point slope data set of Moore and Mark (1986), which was supplied from the U.S. Geological Survey, Menlo Park, California. The data set exists in a spatial resolution of 5' by 5' longitude/ latitude and we averaged it to a resolution of 0.5 degree by 0.5 degree longitude/ latitude.

Lithology

A global map showing the main rock types exposed on the continental areas at present-day has been digitized from synthetic lithological and soil maps published by FAO-UNESCO (1971, 1975, 1976, 1978, 1979, 1981) for each of the continents (Amiotte-Suchet, 1995; Amiotte-Suchet et al., in press). Although the scale of the FAO-UNESCO maps is very tight (about 1/ (50 000 000)), we considered these maps to be sufficient for building up a global numeric map in a 1° by 1° grid point resolution. The FAO-UNESCO maps provide quite complete and precise information about the general lithology of Central and South America, Africa, Asia and Australia, allowing the distinction of carbonate rocks, shales and sands and sandstones among the sedimentary rocks. For North America and Europe, however, the lithological information is often not accurate enough to identify carbonates, shales and sandstones separately. Finally, the FAO-UNESCO maps do not include the Antarctic continent. For this reason, additional information has been collected from various sources. Notably the UNESCO World Geological Atlas of Choubert and Faure-Mauret (1981) has been used to complete the outlines of some geological formations and to build a comprehensive lithologic map for the ice free area of Antarctica. In addition, the paleogeographical maps of Ronov and coworkers (Ronov and Khain, 1961; Khain et al., 1975; Ronov et al., 1979), concerning the

mesozoic and cenozoic periods, have been consulted to complement the lithology of the sedimentary units reported by FAO-UNESCO for Europe and North America.

Since the lithological description of the sedimentary units varies from one source to another, only a few broad categories of rock types were distinguished, which mainly reflect their chemical composition and hence their behavior with respect to chemical weathering. The groups we formed are sands and sandstones, shales, carbonate rocks, combined intrusive igneous rocks and metamorphic rocks (i.e. shield rocks), acid volcanic rocks, and basalts. One of the most important points in the definition of rock categories is the presence of carbonate minerals or not. Weathering rates exponentially increase with the amount of carbonate minerals in rocks. Because of the very large scale at which information has been collected, it cannot be excluded that carbonate minerals are sometimes present in other sedimentary rocks besides just carbonate rocks. For example, the mineralogical composition of shales is highly variable with respect to the presence and the proportion of carbonate minerals. In our work, well-identified carbonate rocks (limestones, dolomites, marls, metamorphic limestones) have been classified as "carbonate rocks" and well-identified non-carbonated clastic sediments have been classified as "sand and sandstones". The remaining "suspect" sedimentary rocks were classified together with argillaceous sedimentary rocks as "shales". Moreover, also evaporitic rocks, which are not clearly identified in our sources (their occurrence is highly variable in space), have been included in the group of shales. This is an obvious problem that should be addressed in the future, since evaporites are easily dissolved and hence significantly affect the river transport of dissolved solids when they are present in their drainage basins. Finally, one has also to mention that the results concerning acid volcanic rocks should be cautiously interpreted because these outcrops are often very small and do not always appear at the scale we worked.

A second lithological map was used for classifying the major rock types on the continents according to their resistance to mechanical erosion. This map was created by Dubus (1989) in a 1 degree by 1 degree longitude/ latitude grid point resolution. He assigned a numerical index (LithMI) to each rock type, with low values indicating high resistance. LithMI ranges from 1 to 40, with 1 = plutonic and metamorphic rocks, 2 = volcanic rocks, 4 = consolidated sedimentary rocks, 10 = different rock types in folded zones, 32 = non-consolidated sedimentary rocks, and 40 = recent alluvial sediments. The map is also described in Probst (1992).

6.2 Spatial Characteristics

6.2.1 Spatial Coverage

All data were created cover the entire continents. Only the polar regions under permanent ice cover were considered to be inactive with respect to continental erosion, which means that in these parts the river fluxes are zero. In reality, this is not necessarily the case, of course. The extension of the polar ice sheets was taken from the data set of Olson et al. (1983; 1985).

The oceanic data indicate all coastal grid points that receive river fluxes from the continents. Note that for a given parameter, the sum of the continental river fluxes (in $Tg\ yr^{-1}$) is greater than the sum of the oceanic fluxes (although the difference is not very large). This is due to the fact that certain parts of the continents are endoreic, which means that they are not drained to the oceans (see [flow_dir.gif](#) image). We determined the extensions of the endoreic parts of the continents by digitizing the limits on topographic maps (Ludwig et al., 1996).

6.2.2 Spatial Resolution

Continent Data Maps: These files are on equal angle Earth grids with spatial resolutions of 0.5 degrees by 0.5 degrees and 1 degree by 1 degree in both longitude and latitude. For the original data sets, we also followed the data set of Olson et al. (1983, 1985) in order to define which of the Earth's grid points belong to the continents, and which belong to the oceans. Since our data were processed on the basis of lower level data, which could have different spatial resolutions, some adjustments were necessary to bring the data to the final 0.5 degrees by 0.5 degrees longitude/ latitude grid point resolution. In the case of finer resolutions, such as for the slope data, we averaged all smaller grids cells being covered by a coarser one (weighted by the grid cell areas, which are slightly variable). In the case of coarser resolutions, such as for our lithological maps, we attributed to all smaller grid cells the value of the coarser one. The data provided here are consistent with the ISLSCP II land/water mask.

Oceanic Data Tables (2.5 x 2 degrees) (not provided with this data set, however there are images provided for the visualization of the data): These original data files were created in a 2.5 by 2.0 degrees longitude/ latitude grid point resolution. This is because the global river routing file we used to bring the river fluxes from the interior of the continents to the drainage basin outlets was defined at this coarse resolution (Miller et al., 1994).

Oceanic Data Maps: These files are on equal angle Earth grids with spatial resolutions of 0.5 degrees by 0.5 degrees and 1.0 degree by 1.0 degree in both longitude and latitude grid point. These files were created by the ISLSCP II staff based on the original oceanic data tables.

6.3 Temporal Characteristics

6.3.1 Temporal Coverage

All fluxes we produced are long-term annual means. No specific period can be attributed to the values. One has nevertheless to say that the values are rather natural values, although it is not excluded that some of the river data we used in our regressions were already influenced by human activities. In the case of river sediment fluxes, where the anthropogenic impact should be greatest due to massive construction of river dams in the second half of the 20th century, we decided to select the literature values referring to the pre-damming situation whenever this information was available. Data on river sediment fluxes after the construction of major dams are scarce and our data hence mainly reflect natural sediment fluxes.

6.3.2 Temporal Resolution

No temporal resolution can be attributed to our data sets.

7. OBSERVATIONS

7.1 Field Notes

Not applicable to this data set.

8. DATA DESCRIPTION

8.1 Table Definition with Comments

Not applicable to this data set.

8.2 Type of Data

8.2.1 Parameter/ Variable Name	8.2.2 Parameter/ Variable Description	8.2.3 Data Range	8.2.4 Units of Measurement	8.2.5 Data Source
1) Continental Flux Data (ASCII Maps)				
F _{DOC}	Fluxes of dissolved organic carbon.	Min=0 Max=19.45 Water=-99	t C km ⁻² yr ⁻¹	model
F _{POC}	Fluxes of particulate organic carbon.	Min=0 Max=95.73 Water=-99	t C km ⁻² yr ⁻¹	model
F _{CO2-RW}	Fluxes of bicarbonate being of atmospheric origin.	Min=0 Max=67.84 Water=-99	t C km ⁻² yr ⁻¹	model
F _{HCO3}	Fluxes of bicarbonate being of atmospheric and of lithological origin	Min=0 Max=135.67 Water=-99	t C km ⁻² yr ⁻¹	model
F _{TSS}	Fluxes of total suspended solids	Min=0 Max=19145 Water=-99	t km ⁻² yr ⁻¹	model
2) Differences Tables (*.dif) (ASCII Tables) (1)				
Lat	Latitude for the center of a cell. South latitudes are negative.	Min=-90 Max=90	Decimal Degrees	Earth Grid
Lon	Longitude for the center of a cell. West longitudes are negative.	Min=-180 Max=180	Decimal Degrees	Earth Grid
Data_Removed	Data value in each cell of the original file that did not match the ISLSCP II land/water mask, and was removed.	Varies by parameter	Varies by parameter	Original Data
Data_Added	Data value for each cell added to the original file because the ISLSCP II land/water mask indicated land, so an interpolated point was added.	Varies by parameter	Varies by parameter	Computed
Interpolation_Level	The number of times the interpolation routine was run to get a precipitation value for this point. The higher the number, the less reliable the value is.	Min=1 Max=4	N/A	Computed
3) Change Map (*_changemap.asc) (ASCII Map) (1)				
Point Changed	Differences between the ISLSCP II land/water mask and the original data: -1 = ISLSCP II mask is water and original data is land (data removed) 0 = Data sets agree over land or water (data unchanged) ≥1 = ISLSCP II mask is land and original data is water or missing (data interpolated)	Min=-1 Max=4	See 8.2.2	Computed

8.3 Sample Data Record

Continent Flux Data

The "differences" files for the continent data are ASCII tables with some header lines, the Lat and Lon coordinates of each point removed, then the value of the data point at that point. At the bottom of the file are the coordinates and data for all points added. See the sample below.

```
ISLSCP-2 Differences for file 'cont_flux_co2rw_hd_map.asc'.
Contains Lat-Lon coordinates and data for each point in the original file
that differed from the ISLSCP-2 Land/Sea mask, and thus was removed.
Points added using interpolation are listed at the bottom of this file.
```

```
Lat,Lon,Data_Removed
83.25,-43.75,0.163
83.25,-43.25,0.162
83.25,-42.75,0.161
83.25,-42.25,0.159
83.25,-41.75,0.158
83.25,-41.25,0.157
"      "
"      "
Lat,Lon,Data_Added,Interpolation_Level
82.75,-63.75,0.4,1
82.75,-63.25,0.6,1
82.75,-47.75,0,1
82.75,-47.25,0,1
82.75,-22.25,0.1,1
```

8.4 Data Format

All of the data files in the ISLSCP Initiative II data collection are in the ASCII, or text format. The map file format consists of numerical fields of varying length, which are delimited by a single space and arranged in columns and rows. The map files at different spatial resolutions each contain the following numbers of column and rows:

- One degree: 360 columns by 180 rows
- 1/2 degree: 720 columns by 360 rows

All files are gridded to a common equal-angle lat/long grid, where the coordinates of the upper left corner of the files are located at 180 degrees W, 90 degrees N and the lower right corner coordinates are located at 180 degrees E, 90 degrees S. Data in the map files are ordered from North to South and from West to East beginning at 180 degrees West and 90 degrees North.

Continental Flux Data Set

Oceanic or water grid points are assigned the value -99. All parts of the continents which are covered by ice have specific carbon and sediment fluxes of 0.000.

The ASCII 1/2 degree map files (with the extension of ".asc") have all had the ISLSCP II land/water mask applied to them. All points removed from the original files are stored in "differences" files (with the extension ".dif"). These ASCII table files contain the Latitude and Longitude location of the cell-center of each point from the precipitation that don't match the ISLSCP II land/water mask, and were removed. At the bottom of each file is also a list of all points added to the file through "nearest neighbor averaging" interpolation (see Section 9.2.3), where the land/water mask indicated land but there was no data in the original file (if there were no "neighbor" pixels with data, the missing data was assigned a value of -88). There is also a

column called "Interpolation_Level" that contains the number of times the interpolation routine was run to get a value for that point. The higher the number, the less reliable the value is. There is one ".dif" file for each ASCII 1/2 degree map file.

The "change map" file shows the results of applying the land/water mask, as a viewable ASCII map: all points added (positive number, containing the "Interpolation_Level", see above), all points unchanged ("0"), and all points removed ("-1"). There is only a half-degree map.

WARNING: The 1x1 degree Continent product is recommended for browse use. These data files are averaged from the original 0.5 x 0.5 degree map files. Thus the data values at specific pixels are not exact. Use this data with caution and always refer to the original half-degree data files for specific information.

8.5 Related Data Sets

A previous release of our data for the atmospheric CO₂ consumption by rock weathering ($F_{\text{CO}_2\text{-RW}}$) is available via the internet from the Carbon Dioxide Information Analysis Center (CDIAC) server (Amiotte-Suchet and Probst, 1995b – see web site address in the reference list under Section 12.2). These data were created in a 1degree by 1degree longitude/latitude grid point resolution by using a different lower level data set for drainage intensity.

The ISLSCP II data collection contains many recent versions of many of the same input data used to create these data sets. Examples include the Simulated Topological Network (STN) for river routing, various precipitation data sets, the HYDRO1k elevation and elevation-derived products, and the International Geosphere-Biosphere Programme (IGBP) soils data set, among others. Additional [ISLSCP II](#) data sets are also available from the Oak Ridge National Laboratory Distributed Active Archive Center ([ORNL DAAC](#)).

9. DATA MANIPULATIONS

9.1 Formulas

9.1.1 Derivation Techniques/Algorithms

A) Inorganic Carbon Fluxes

The inorganic carbon fluxes in GEM-CO₂ were calculated on the basis of the grid point lithology and the corresponding drainage intensity according to the following set of equations. The units are t C km⁻² yr⁻¹ for the carbon fluxes ($F_{\text{CO}_2\text{-RW}}$ and F_{HCO_3}) and mm for the drainage intensity.

sands and sandstones	$F_{\text{CO}_2\text{-RW}} = 0.001824 \times Q$	(4)
----------------------	---	-----

	$F_{\text{HCO}_3} = 0.001824 \times Q$	(5)
--	--	-----

carbonates	$F_{\text{CO}_2\text{-RW}} = 0.019032 \times Q$	(6)
------------	---	-----

	$F_{\text{HCO}_3} = 0.038064 \times Q$	(7)
--	--	-----

$$\text{shales} \quad F_{\text{CO}_2\text{-RW}} = 0.007524 \times Q \quad (8)$$

$$F_{\text{HCO}_3} = 0.007524 \times Q \quad (9)$$

$$\text{plutonic and metamorphic rocks} \quad F_{\text{CO}_2\text{-RW}} = 0.001140 \times Q \quad (10)$$

$$F_{\text{HCO}_3} = 0.001140 \times Q \quad (11)$$

$$\text{basalts and gabbros} \quad F_{\text{CO}_2\text{-RW}} = 0.005748 \times Q \quad (12)$$

$$F_{\text{HCO}_3} = 0.005748 \times Q \quad (13)$$

$$\text{acid volcanic rocks} \quad F_{\text{CO}_2\text{-RW}} = 0.002664 \times Q \quad (14)$$

$$F_{\text{HCO}_3} = 0.002664 \times Q \quad (15)$$

B) Organic Carbon Fluxes

Dissolved organic carbon fluxes (F_{DOC}) were determined on the basis of the grid point values for the drainage intensity (Q), for the steepness of morphology (Slope) and of the organic carbon content in the soil (SoilC) according to a multiple correlation model with the following equation:

$$F_{\text{DOC}} = 0.0044 \times Q - 8.49 \times \text{Slope} + 0.0581 \times \text{SoilC} \quad (16)$$

The units of the parameters are as follows: $F_{\text{DOC}} = \text{t C km}^{-2} \text{ yr}^{-1}$; $Q = \text{mm}$; Slope = radian; and SoilC = kg/m^3 .

For the fluxes of particulate organic carbon (F_{POC}), it is the total suspended sediment flux (F_{TSS}) that is the most important controlling factor. The percentage of particulate organic carbon in the riverine suspended solids (POC%) generally decreases with increasing sediment concentrations (TSS) following a non-linear relationship. We fitted this relationship with the following three-order polynomial equation:

$$\text{POC}\% = -0.160 \times \log(\text{TSS})^3 + 2.83 \times \log(\text{TSS})^2 - 13.6 \times \log(\text{TSS}) + 20.3 \quad (17)$$

The units are % for POC% and mg/l for TSS. An extrapolation of POC fluxes over the continents requires thus the availability of a global data set for sediment fluxes (see below) and of drainage intensity. This allows determining an average river sediment concentration per grid cell, from which the corresponding POC% value can be derived according to equation (17). The final flux of POC (in $\text{t C km}^{-2} \text{ yr}^{-1}$) is then calculated with:

$$F_{\text{POC}} = \text{POC}\% \times F_{\text{TSS}} \quad (18)$$

C) River Sediment Fluxes

Sediment fluxes (F_{TSS}) can be predicted best by correlating them with the products of hydroclimatic, geomorphological, and lithological factors, that is drainage intensity (Q), basin slope, our index characterizing rock hardness (LithMI), and our index characterizing rainfall variability over the year (Four). The best correlated parameter combination is dependent on climate, and the following set of equations was used to create a data set on the spatial distribution of river sediment yields on the continents:

$$\begin{array}{l} \text{Tundra \& taiga climate,} \\ \text{polar climate} \end{array} \quad F_{TSS} = 0.125 \times \text{Slope} \times Q \times \text{LithMI} \quad (19)$$

$$\text{Temperate wet climate} \quad F_{TSS} = 16.25 \times \text{Four} \times \text{Slope} \quad (20)$$

$$\text{Tropical wet climate} \quad F_{TSS} = 0.00081 \times \text{Four} \times \text{Slope} \times Q \times \text{LithMI} \quad (21)$$

$$\text{Dry climates (temperate} \\ \text{dry, tropical dry, desert)} \quad F_{TSS} = 0.01176 \times \text{Four} \times \text{Slope} \times Q \times \text{LithMI} \quad (22)$$

The units of the parameters are as follows: $F_{TSS} = t \text{ km}^{-2} \text{ yr}^{-1}$; Q = mm; Slope = radian and Four = mm; LithMI is without unit.

9.2 Data Processing Sequence

9.2.1 Processing Steps and Data

Since all lower level data exist in a 0.5 degree by 0.5 degree grid point resolution, all calculations to produce our continental data sets were done on the level of the individual continental grids cells by applying to above-explained equations.

The oceanic data sets were created by superimposing the continental data sets on the river routing file of Miller et al. (1994). Because of the coarser resolution, the total continental area defined by the routing file is lower than the area of the continental data sets. In the routing files, the coastal morphologies are much simplified and smaller islands cannot be represented. Whenever the routing file was used to bring the river carbon fluxes to the oceans, we retained first the fluxes within the limits of our endoreic part of the continents, and then superimposed the remaining fluxes on the routing files in a way that no carbon and sediments was 'lost' through the change in resolution.

9.2.2 Processing Changes

We should mention that in some of our older publications, some the lower level data sets used to run GEM-CO₂ were different from those we described here. This could lead to different results with respect to the global and regional budgets we give here, although the differences are only small.

9.2.3 Additional Processing by the ISLSCP Staff

Continental Flux Data

The original data files submitted to the ISLSCP staff came in a variety of formats. The original Continent map files were at half-degree, and had 10 values per line, a blank line between each data line, and the origin of the images was at 90 degrees S. Missing data were encoded as "-999.00". These files were first processed to remove the blank

lines, then reprocessed where 36 lines were concatenated into one, the missing values were set to "-99", and the origin changed to 90 degrees N, creating the half-degree product. These files were then processed again, averaging each cluster of 4 0.5 degree cells into one degree cells to create the 1.0 degree product.

The ISLSCP II staff then processed the ASCII Continent map files by comparing them against the ISLSCP II land/water mask. Missing land data in these files were replaced through "nearest neighbor averaging" interpolation. New ASCII table files containing the removed and added points (points that didn't match the land/water mask), also called "differences" files with the extension ".dif", were also created for the half-degree data (they were not needed for the 1-degree data, as this had been averaged from the half-degree data). These files contain the Latitude and Longitude of the cell-center of each point removed from the continental flux maps, and the value removed from each map. At the bottom of the file are the added continental flux points, and a column called "Interpolation_Level" that contains the number of times the interpolation routine was run to get a value for that cell. The higher the number, the less reliable the value is.

Finally, a "change map" was created for the half-degree data, showing the results of applying the land/water mask, as a viewable ASCII map: all points added (positive number, containing the "Interpolation_Level", see above), all points unchanged ("0"), and all points removed ("-1"). Users can use the data, the ".dif" files and the change map to re-create the original data set as it was submitted by the Principal Investigator.

9.3 Calculations

9.3.1 Special Corrections/Adjustments

In general, the spatial distribution of the river sediment yields we produced with our empirical models depicts a regional variability that is in good agreement with field data (for a review of literature estimates, see Ludwig and Probst, 1998). Nevertheless, some outstanding features, such as the very high sediment yields in the Yellow river basin in China, cannot be reproduced with our models. For this reason we performed a correction of this data by coupling our modeled values with the observed values for the rivers for which we had literature data. This concerned 60 major world rivers that cover together about half of the total endoreic and ice-free continental area.

Within the borders of the river basins for which we had field data, we corrected all grid point values according to:

$$F_{TSS} \text{ (corrected)} = F_{TSS} \text{ (modeled)} \times \frac{F_{TSS} \text{ (basin average, observed)}}{F_{TSS} \text{ (basin average, modeled)}} \quad (23)$$

For the grid points that do not fall into one of our basins, the values were obtained by a triangular interpolation between the next basin values. Also the interpolation was coupled to the modeled values according to:

$$F_{TSS} \text{ (corrected)} = F_{TSS} \text{ (corrected, interpolated)} \times \frac{F_{TSS} \text{ (modelled)}}{F_{TSS} \text{ (modelled, interpolated)}} \quad (24)$$

The created data set is not much different from our purely modeled data set, but it better reflects some regional and local patterns (Ludwig and Probst, 1998). We therefore

considered this map to be the best representation of the global distribution of river sediment yields that can be made on the basis of our data.

9.4 Graphs and Plots

For the oceanic flux data, we have supplied a GIF image file showing the global distribution of the data in a map. Consequently, there are 10 maps corresponding to the 10 data sets. An 11th map shows the global river routing file ([flow_dir.gif](#)) that has been used to bring the river fluxes from the interior of the continents to the oceans (Miller et al., 1994). This routing file has not been created by us, and it is not included in numerical form in the data sets.

10. ERRORS

10.1 Sources of Error

Since we computed our data on the basis of lower spatial resolution data sets, the reliability of our data naturally depends strongly on the quality of the input data. A more general problem of our approach is the fact that the data we produced are based on the assumption that the fluxes are conservative with respect to the river transport. This is less problematic for the fluxes of the dissolved species, although here also modifications during the transport can occur (e.g., mineralization of DOC in the rivers, precipitation of carbonate in lakes, etc.). But it is evident that, as far as the fluxes of particulate matter are concerned (F_{TSS} and F_{POC}), our approach suffers from the shortcoming that it cannot account for sediment storage in the river basins. The continental data sets we created should therefore have a tendency to smooth local variability. Storage in one part of the basin must be compensated by greater erosion rates in another part of the basin to yield the average sediment flux observed at the river mouth. This means that in reality, the variability of the river fluxes on the continents may be more important as predicted by our empirical models, and that erosion may be much greater as this is shown by our data.

10.2 Quality Assessment

10.2.1 Data Validation by Source

Validation of our model outputs was done by comparing the global and regional budgets we produced with independent literature estimates that have been established by different methods. In general, we found a good agreement with this. An important question in our approach is whether the data we used to establish our empirical models are representative at the global scale or not. We always examined very thoroughly this question when selecting the river data out of the literature (see our papers).

10.2.2 Confidence Level/Accuracy Judgment

It is evident that including different river data in the regression statistics might slightly change the regression coefficients, and hence also the model outputs. In establishing our regression models much time has been spent to test the sensitivity of the models with respect to this. Most of the models are simple linear regression models that are quite robust in this sense. The only case where our regressions are sensitive to changes of the input parameters concerns our models for river sediment yields. Here, the fluxes are correlated to the products of different parameters. Changing the parameter combinations can have a considerable impact on the model outputs without much change to the correlation coefficients. In our case, this concerns mainly our index for the

characterization of rock hardness with respect to mechanical erosion (LithMI). Omitting this parameter from the regressions would result in a global sediment discharge to the oceans of about 18.5 Gt yr^{-1} , instead of 16 Gt yr^{-1} as we propose here (for a more detailed discussion, see Ludwig and Probst, 1998). It has therefore to be kept in mind that our values for the particulate matter fluxes may be too low.

Another case where the fluxes produced by GEM-CO₂ might be too low concerns the fluxes of inorganic carbon ($F_{\text{CO}_2\text{-RW}}$ and F_{HCO_3}). In our approach, these fluxes are exclusively determined as a function of rock type and of drainage intensity. The impact of other potential controlling factors could not be parameterized, although it has often been proposed that climatic factors, especially temperature, should have a considerable influence on the atmospheric CO₂ consumption by chemical weathering and on the river bicarbonate fluxes. In Ludwig et al. (1998) we tested whether there might be a dependency of the reliability of the model output on climate and found that there might be a tendency to underestimate the fluxes in the mid and higher latitudes. Globally, this underestimation could be in the range of one third of the overall fluxes. In the above-mentioned paper, we also proposed a procedure to correct this underestimation, leading to different data sets as the ones we present here. On interest, these data sets could be supplied when contacting us.

10.2.3 Measurement Error for Parameters and Variables

All data sets we produced are model outputs. They were produced by combining different empirical regression models that have been established at different levels (small and large river basins), and on the basis of different numbers of observations. The attribution of error bars to the values we calculated is not possible.

10.2.4 Additional Quality Assessment Applied

None.

11. NOTES

11.1 Known Problems with the Data

None reported at this revision

11.2 Usage Guidance

See Section 10 and the references given for a discussion of the limitations of these data sets. Users should be aware that all data sets provided here are model outputs. They were produced by combining different empirical regression models that have been established at different levels (small and large river basins), and on the basis of different numbers of observations. We also note that in some of our older publications, some the lower level data sets used to run GEM-CO₂ were different from those we described here. This could lead to different results with respect to the global and regional budgets we give here, although the differences are only small.

The ISLSCP II staff has modified the original data sets in order to provide consistency with land/water boundaries throughout the entire collection. This may also change global or continental totals from the original data. The ISLSCP II staff has also produced both coarser (1.0

degree continent flux) and higher spatial resolution (0.5 and 1.0 degree oceanic flux) data from the original data. We recommend these data for browse use. Users are urged to use and consult the original data sets as much as possible.

11.3 Other Relevant Information

None.

12. REFERENCES

12.1 Satellite/Instrument/Data Processing/ Lower Level Data Documentation

- Ahamer, G., Spitzer, J., Weiss, C.O. and Fankhauser, G., 1992. *Der Einfluß einer verstärkten energetischen Biomassennutzung auf die CO₂-Konzentration in der Atmosphäre*. Abschlussbericht. Institut für Energieforschung, Joanneum Research, Graz.
- Choubert, G., and A. Faure-Mauret, 1981 ; *Atlas géologique du monde*, Commision de la Carte Géologique du Monde, Bureau de Cartographie Géologique Internationale, UNESCO, Paris, 32 sheets.
- Claussen, M., Lohman, U., Roeckner, E. and Schulzweida, U., 1994. *A global data set of land-surface parameters*. MPI report 135, Max-Planck-Institut für Meteorologie, Hamburg, 23 pp.
- CORINE, 1992. *Soil Erosion Risk and Important Land Resources in the Southern Regions of the European Community*. Report EUR 13233, Office for Official Publications of the European Communities, Brussels, 99 pp.
- Degens, E.T., Kempe, S. and Richey, J.E., 1991. *Biogeochemistry of Major World Rivers*. SCOPE Rep. 42. John Wiley, New York, pp. 356.
- Dubus, P., 1989. *Paramétrisation des grands bassins fluviaux du monde. Modélisation de l'érosion mécanique et de l'érosion chimique des continents*. Mém. de DEA, Université Louis Pasteur, Strasbourg, 30 pp.
- UNESCO/ FAO (Food and Agriculture Organization/ U.N. Educational, Scientific, and Cultural Organization), 1971, 1975, 1976, 1978, 1979, 1981. *Soil map of the World. Vol. I to Vol. X*. UNESCO Press, Paris.
- FNOC (Fleet Numerical Oceanography Center), 1992. *Global elevation, terrain, and surface characteristics. Digital raster on a 10 minute geographic (lat/long) 1080x2160 grid*. In: NOAA/ National Geophysical Data Center (Editor), *Global Ecosystems Database, Version 1.0 Disc (CD-ROM)*. National Geophysical Data Center, Boulder, Colorado.
- Fournier, F., 1960. *Climat et érosion*. Presses Universitaires de France, Paris, 201 pp.
- Holdridge, L.R., 1947. Determination of world plant formations from simple climatic data. *Science*, 105, 367-368.
- Holdridge, L.R., 1959. Simple method for determining potential evapotranspiration from temperate data. *Science*, 130, 572.
- Khain, V.E., A.B. Ronov, and A.N. Balukhovskiy, 1976. Cretaceous lithologic associations of the world, *International Geology Review*, Engl. Transl., 18, 1269-1295.
- Korzoun, V.I., Sokolov, A.A., Budyko, M.I., Voskresensky, G.P., Kalinin, A.A., Konoplyantsev, E.S., Korotkevich, E.S. and Lvovich, M.I., 1977. *Atlas of World Water Balance*. UNESCO Press, Paris, 36 pp.
- Legates, D.R. and Willmott, C.J., 1992. *Monthly average surface air temperature and precipitation: Digital raster on a 30-minute geographic (lat/long) 360x720 grid*. In: NOAA/

- National Geophysical Data Center (Editor), Global Ecosystems Database, Version 1.0 Disc (CD-ROM). National Geophysical Data Center, Boulder, Colorado.
- Meybeck, M., 1986. Composition chimique des ruisseaux non pollués de France. *Sci. Géol. Bull.*, 39, 3-77.
- Moore, J.G. and Mark, R.K., 1986. World slope map. *EOS Trans. AGU*, 67, 1353-1356.
- Olson, J.S., Watts, J.A. and Allison, L.J., 1983. *Carbon in live vegetation of major world ecosystems*. Report ORNL-5862, Oak Ridge Laboratory, Oak Ridge, Tennessee, 164 pp.
- Olson, J.S., Watts, J.A. and Allison, L.J. 1985. *Major world ecosystem complexes ranked by carbon in live vegetation: A database*, Rep. NDP-017. Carbon Dioxide Information Analysis Center, Oak Ridge Nat. Laboratory, Oak Ridge, Tennessee, 19 pp.
- Post, W.M (1993) *Organic carbon in soil and the global carbon cycle*. In: M. Heimann (ed.) *The global Carbon Cycle*. NATO ASI Series I., Vol. 15. Springer, Berlin Heidelberg, 599 pp.
- Probst, J.L., 1992. *Géochimie et hydrologie de l'érosion continentale. Mécanismes, bilan global actuel et fluctuations au cours des 500 derniers millions d'années*. *Sci. Géol. Mém.*, Strasbourg, 94, 161 pp.
- Ronov, A.B., and V.E. Khain, 1961. Triassic lithologic association of the World (in Russian), *Sovetskaya Geologiya*, 1, 32-46.
- Ronov, A.B., V.E. Khain, and A.N. Balukhovskiy, 1979. Paleogene lithologic associations of the continents, *International Geology Review*, Engl. Transl., 21, 415-446.
- Webb, R.S., Rosenzweig, C.E. and Levine, E.R., 1991. *A global data set of soil particle size properties*. NASA Technical Memorandum, # 4286. NASA, Washington D.C., 33 pp.

12.2 Journal Articles and Study Reports on the Data Sets

- Amiotte-Suchet, P. and Probst, J.L., 1993a. Modeling of atmospheric CO₂ consumption by chemical weathering of rocks: Application to the Garonne, Congo and Amazon basins. *Chemical Geology*, 107, 205-210.
- Amiotte-Suchet, P. and Probst, J.L., 1993b. Flux de CO₂ consommé par altération chimique continentale: influence du drainage et de la lithologie. *C. R. Acad. Sci. Paris*, 317, 615-622.
- Amiotte-Suchet, P., 1995. *Cycle du carbone, érosion chimique des continents et transferts vers les océans*. *Sci. Géol. Mém.*, Strasbourg, 97, 156 pp (in French).
- Amiotte-Suchet, P. and Probst, J.L., 1995a. A global model for present day atmospheric/ soil CO₂ consumption by chemical erosion of continental rocks (GEM-CO₂). *Tellus*, 47B, 273-280.
- Amiotte-Suchet, P. and Probst, J.L., 1995b, *A Global 1 Degree by 1 Degree Distribution of Atmospheric/Soil CO₂ Consumption by Continental Weathering and of Riverine HCO₃ Yield* CDIAC DB-1012, <http://cdiac.esd.ornl.gov/ndps/db1012.html>.
- Amiotte-Suchet, P., Probst, J.L., and Ludwig, W. (in press). Worldwide distribution of continental rock lithology: implications for the atmospheric/soil CO₂ uptake by continental weathering and alkalinity river transport to the oceans. *Global Biogeochemical Cycles*, in press.
- Aumont, O., Orr, J.C., Monfray, P., Ludwig, W., Amiotte-Suchet, P., and Probst, J.-L. (2001) Riverine-driven interhemispheric transport of carbon. *Global Biogeochemical Cycles*, 15, 393-405.
- Ludwig, W. and Probst, J.L., 1996. *A global modeling for the climatic, morphological, and lithological control of river sediment discharges to the oceans*. In: D.E. Walling and B.W. Webb (Editors) *Erosion and Sediment Yield: Global and Regional Perspectives*. Proceedings on the Exeter Symposium. IAHS Publ. no. 236, IAHS Press, Wallingford, 21-28.

- Ludwig, W., Probst, J.-L., and Kempe, S. (1996a). Predicting the oceanic input of organic carbon by continental erosion. *Global Biogeochemical Cycles*, 10, p. 23-41.
- Ludwig, W., Amiotte-Suchet, P., and Probst, J.-L. (1996b). River discharges of carbon to the world's oceans: Determining local inputs of alkalinity and of dissolved and particulate organic carbon. *C. R. Acad. Sci. Paris*, 323, p. 1007-1014.
- Ludwig, W. (1997). *Continental erosion and river transport of organic carbon to the world's oceans*. Mém. Sciences Géologiques, Strasbourg, 98, 196 pp (in English).
- Ludwig, W., and Probst, J.-L. (1998). River sediment discharge to the oceans: Present-day controls and global budgets. *American J. Science*, 296, p. 265-295.
- Ludwig, W., Amiotte-Suchet, P., Munhoven, G., and Probst, J.-L. (1998). Atmospheric CO₂ consumption by continental erosion: Present-day controls and implications for the last glacial maximum. *Global and Planetary Change*, 16, p. 95-108.
- Ludwig, W., Amiotte-Suchet, P., and Probst, J.-L. (1999). Enhanced chemical weathering of rocks during the last glacial maximum: a sink of atmospheric CO₂? *Chem. Geology*, 159, p. 147-161.
- Ludwig, W., and Probst, J.-L. (1999). Soil erosion and atmospheric CO₂ during the last glacial maximum : the role of riverine organic matter fluxes. *Tellus* 51B, p. 156-164.
- Miller, J.R., Russell, G.L. and Caliri, G., 1994. Continental-scale river flow in climate models. *J. Climate*, 7, 914-928.

13. DATA ACCESS

13.1 Contacts for Archive/Data Access Information

The ISLSCP Initiative II data are available are archived and distributed through the Oak Ridge National Laboratory (ORNL) DAAC for Biogeochemical Dynamics at <http://daac.ornl.gov>.

13.2 Contacts for Archive

E-mail: uso@daac.ornl.gov
Telephone: +1 (865) 241-3952

13.3 Archive/Status/Plans

The ISLSCP Initiative II data are archived at the ORNL DAAC. There are no plans to update these data.

14. GLOSSARY OF ACRONYMS

ABT	Average Biotemperature
APE	Annual Potential Evapotranspiration
APETR	Annual Potential Evapotranspiration Ratio
APPT	Annual Precipitation Total
CDIAC	Carbon Dioxide Information Analysis Center
CEFREM	Centre de Formation et de Recherche sur l'Environnement Marin

CNRS	Centre National de la Recherche Scientifique (France)
DAAC	Distributed Active Archive Center
DAAC	Distributed Active Archive Center
DIC	Dissolved inorganic carbon
DOC	Dissolved organic carbon
ESCOBA	European Study of Carbon in the Ocean, Biosphere and Atmosphere
FAO	Food and Agriculture Organization (U.N.)
F _{CARB}	Fluxes of bicarbonates being of lithological origin (carbonates)
F _{CO2-RW}	Fluxes of bicarbonates being of atmospheric origin
F _{DOC}	Fluxes of dissolved organic carbon
F _{HCO3}	Fluxes of total bicarbonates (lithological and atmospheric origin)
FNOC	Fleet Numerical Oceanography Center
F _{POC}	Fluxes of particulate organic carbon
F _{TSS}	Fluxes of total suspended solids
GEM	Global Erosion Model
GSFC	Goddard Space Flight Center
IGBP	International Geosphere-Biosphere Programme
ISLSCP	International Satellite Land Surface Climatology Project
NASA	National Aeronautics and Space Administration
ORNL	Oak Ridge National Laboratory
POC	Particulate organic carbon
Q	Drainage intensity (runoff divided by basin area)
SCS	Soil Conservation Service (USDA)
STN	Simulated Topological Network
TSS	Total suspended solids (sediments)
UNEP	United Nations Environment Program
USDA	United States Department of Agriculture
USGS	United States Geological Survey